Scientia Iranica B (2020) 27(1), 341–349

Sharif University of Technology
Scientia Iranica
Transactions B: Mechanical Engineering
http://scientiairanica.sharif.edu

Comparative study of damage behavior of synthetic and natural fiber-reinforced brittle composite and natural fiber-reinforced flexible composite subjected to low-velocity impact

M. Vishwas*, **S. Joladarashi, and S.M. Kulkarni**

Department of Mechanical Engineering, National Institute of Technology Karnataka, Surathkal, Mangaluru 575025, India.

Received 23 June 2018; received in revised form 18 September 2018; accepted 29 October 2018

KEYWORDS
Rubber;
Damage;
Energy absorbed;
Glass fiber;
Jute fiber;
Low-velocity impact;
Stiff and flexible composites.

Abstract. In the present study, a comparative study of the damage behavior of Glass-Epoxy (GE), Jute-Epoxy (JE) laminates with $[0/90]_s$ orientation, and Jute-Rubber-Jute (JRJ) sandwich is carried out by ABAQUS/CAE finite element software. The GE, JE laminate, and JRJ sandwich with a thickness rate of 2 mm are impacted by a hemispherical-shaped impactor at a velocity of 2.5 m/s. The mechanisms by which the brittle laminate gets damaged are analyzed in accordance with Hashin's 2D failure criterion, and flexible composites are analyzed by the ductile damage mechanism. The absorbed energy and the incipient point of each laminate were compared. According to the results, there was no evidence of delamination in JRJ as opposed to GE and JE. The compliant nature of a rubber plays a role in absorbing more energy, which is slightly higher than the energy absorbed in GE. Moreover, it was observed that there was no incipient point in JRJ sandwich, meaning that there was no cracking of matrix since the rubber was elastic material. Thus, the JRJ material can be a better substitute for GE laminate in low-velocity applications. The procedure proposed for the analysis in the present study can serve as a benchmark method for modeling the impact behavior of composite structures in further investigations.

1. Introduction

In the field of automobiles, most of the fuel consumption is directly dependent on the vehicle's weight. Thus, in terms of environment and economy, the reduction of the vehicle's weight is of greater interest, as pointed out by Friedrich and Almajid [1]. Out of various alternatives available in reducing the weight of a vehicle, the most popular method is using Fiber-Reinforced Plastic (FRP) composites instead of metals and alloys. The specific stiffness and strength of FRP composites are superior to those of metals, thus making them potential candidates for structural applications in automotive. However, according to Dogan and Arikan [2], the application of FRPs is still a matter of concern as they are highly prone to internal damage due to external dynamic loads such as Low-Velocity Impact (LVI: defined as events in the velocity range of 1-10 m/s).

According to Richardson and Wisheart [3], before deciding upon the use of the FRPs in structural components, predicting the damage under impact load is a critical issue as the structural integrity of the component can be reduced due to impact loading. Damages such as matrix cracking and delamination

*. *Corresponding author.*
E-mail address: vishwasmahesh@gmail.com (M. Vishwas)

doi:10.24200/sci.2018.51294.2100

are expected in the FRPs subjected to LVI, which are barely visible through visual inspection, and it appears that the component is undamaged [4-6]. Hence, to prevent the catastrophic failure of the components made by FRP composites, the study of the behavior of FRP composites subjected to LVI has received considerable attention [2,7-10].

Engineers in almost all industries are using synthetic fibers, such as Glass-Epoxy (GE) and Carbon-Epoxy (CE), to reduce the weight of the component [11,12]. However, brittleness is the drawback of such fibers that makes them low-impact damage-resistant materials, pulling their candidature back in impact dynamics [13-17]. Owing to environmental and energy concerns, researchers are losing interest in synthetic fibers [18,19]. Natural fibers are slowly taking over synthetic fibers in almost all industries. The automotive industry has already started using the components made by natural fibers, especially in their interior parts [20,21]. Apart from benefits such as low cost and environmental concerns, naturally available fibers also possess some technical benefits. Compared to brittle glass fibers, resistance to the impact of brittle fibers is an important advantage.

Of all the various natural fibers available for usage in composites, the most investigated natural fiber is jute, which is extracted from *Corchorus capsularis* plant. According to a study carried out by Satyanarayana et al. [22], jute consists of 60% cellulose, 22% hemi-cellulose, and 16% lignin. Though jute provides useful mechanical properties to become a potential reinforcement material in composite, some of the properties require further evaluations before finalizing its application.

Ariatapeh et al. [23] argued that high cost and long time involved in sample preparation, manufacturing, and testing made the application of numerical methods inevitable as a preliminary step. Since the present study is a preliminary step toward exploring the application of the new material for energy absorption application under LVI, an analysis is performed by the Finite Element Method (FEM). The present study carries out the numerical analysis of GE and JE laminates with a stacking sequence $[0/90]_s$ and compares them with JRJ sandwich to determine the suitability of the fiber for LVI applications. According to Vishwas et al. [24], using a rubber in the composite would enhance the energy absorption ability of the composite. The nature of damages in GE, JE, and JRJ is analyzed.

2. Mesh convergence and verification of the FE model

The present section deals with the mesh convergence study and verifying the FE model. The FE tool is used in the present study to validate the results obtained by Karas [25]. Hyunbum [26] used the same reference to validate his study on graphite-epoxy composite. To this end, the example considered by Karas [25] is reproduced with the aid of the presented methodology.

Karas [25] considered a steel plate of 0.2 m $\times$ 0.2 m $\times$ 0.008 m dimension with fixed edges being impacted by a steel ball of 0.01 m in diameter with a velocity of 1 m/s.

Figure 1 shows the plate and the impactor reproduced similar to that presented by Karas [25]. Quadratic element S4R (a 4-node doubly curved thin or thick shell, reduced integration, hourglass control, and finite membrane strains) and R3D4 (a 4-node 3-D bilinear rigid quadrilateral) are used for meshing the plate and ball, respectively. In the present study, the total number of elements and nodes used is 1982 and 2064, respectively. In order to select a better mesh size with regard to the convergence and computational efficiency, a mesh convergence study has been carried out with a series of mesh sizes ranging from 0.5 mm to 2.5 mm with an increment rate of 0.5 mm.

The results obtained by the FE method are compared with the analytical results obtained by Karas [25], as shown in Figure 2. By observing the variation of contact force and deformation against time, it can be concluded that the results of the present method adopted through FE simulation closely are in

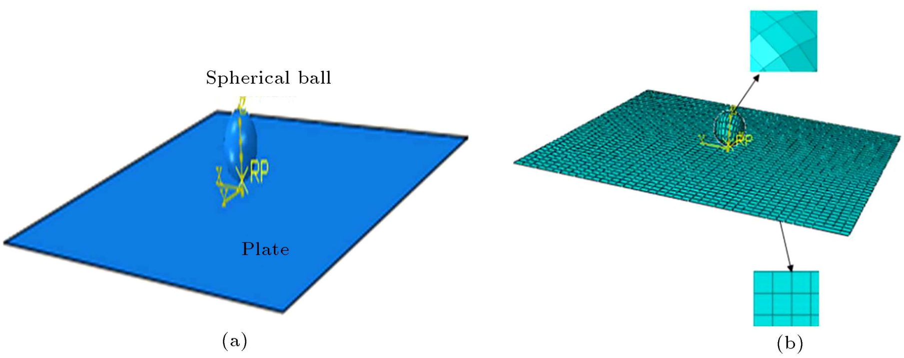

Figure 1. (a) Modeling and (b) meshing of the plate and spherical ball.

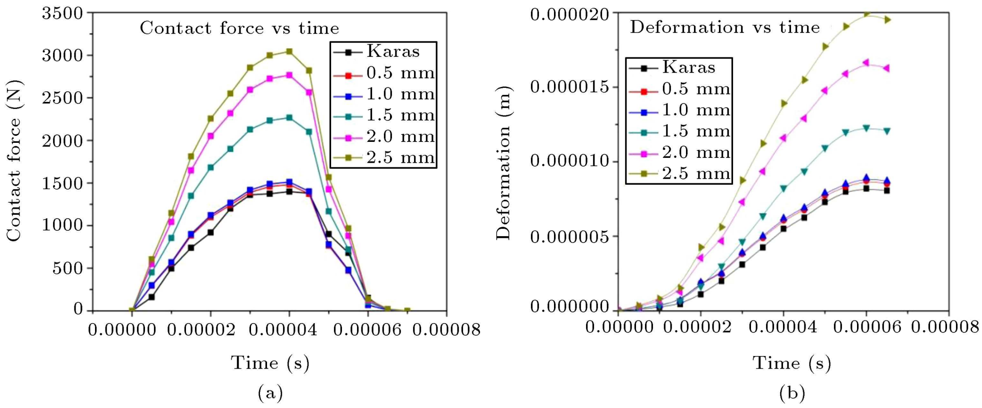

Figure 2. Variation of (a) contact force and (b) deformation of the plate as a function of time (intended for colour reproduction).

Table 1. Material properties of GE and JE.

Material	ρ (kg/m^3)	E_1 (GPa)	$E_2 = E_3$ (GPa)	$G_{12} = G_{13}$ (GPa)	G_{23} (GPa)	X_t (GPa)	X_c (GPa)	Y_t (GPa)	Y_c (GPa)
GE	1635	30.5	4.02	2.08	1.44	0.686	0.270	0.035	0.088
JE	1337.5	4.5	3.2	1.45	1.63	0.104	0.102	0.011	0.095

agreement with those of Karas [25] when the mesh size chosen is 1 mm. Hence, it is concluded that the finite element method applied in this study enjoys validity with a mesh size of 1 mm.

3. Material properties and numerical modeling

3.1. Material properties

GE, JE laminates along with JRJ sandwich composite plates are considered in the present study. The properties of GE, JE, and JRJ are derived from [27-32]. Table 1 gives the material properties of GE and JE, and Table 2 gives the properties of jute and rubber.

3.2. Modeling of laminate failure

The present study applies Hashin's failure criterion to anticipate the failure of composite laminate used in the present study. Hashin's 2D criterion is inbuilt in ABAQUS and works only with shell elements (SC8R). Eqs. (1)-(4) produce the four failure modes considered during the analysis:

Fiber tension ($\hat{\sigma_{11}} \geq 0$):

$$F_f^t = \left(\frac{\hat{\sigma_{11}}}{X^t}\right)^2 + \alpha \left(\frac{\hat{\sigma_{12}}}{S^L}\right)^2. \tag{1}$$

Fiber compression ($\hat{\sigma_{11}} \leq 0$):

$$[C_d]F_f^c = \left(\frac{\hat{\sigma_{11}}}{X^c}\right)^2. \tag{2}$$

Table 2. Material properties of jute and rubber.

	Density (kg/m^3)	Youngs modulus (GPa)	Poissons ratio
Jute	1450	20	0.38
Rubber	1060	Neo Hookean parameters: C_{10}: 16.77E9 Pa, D_1: 1.2E-9 Pa^{-1}	

Matrix tension ($\hat{\sigma_{22}} \geq 0$):

$$F_m^t = \left(\frac{\hat{\sigma_{22}}}{Y^t}\right)^2 + \left(\frac{\hat{\sigma_{12}}}{S^L}\right)^2. \tag{3}$$

Matrix compression ($\hat{\sigma_{22}} \leq 0$):

$$F_m^c = \left(\frac{\hat{\sigma_{22}}}{2S^T}\right)^2 + \left[\left[\frac{Y^C}{2S^T}\right]^2 - 1\right]\left(\frac{\hat{\sigma_{22}}}{Y^C}\right) + \left(\frac{\hat{\sigma_{12}}}{S^L}\right)^2. \tag{4}$$

In Eqs. (1)-(4), $\hat{\sigma_{ij}}(i,j = 1,2)$ represents the effective stress tensor components. The tensile and compressive strengths of the laminate are represented by X^t, X^c in the longitudinal direction and Y^t, Y^c in the transverse direction. The in-plane and out-of-plane shear strengths of the laminate are represented by $S^j(j = L,T)$. The material, before damage initiation, will behave linear elastic during which the stress-strain can be related as in $\{\sigma\} = [C]\{\varepsilon\epsilon\}$, where $[C]$ is the elasticity matrix that changes into the damage elasticity matrix $[C_d]$ once the damage is initiated. The damage elasticity matrix is defined by Eq. (5) as shown in Box I. In Eq. (5) $D = 1-(1-d_f)(1-d_m)\gamma_{12}\gamma_{21}$ and

$$[C_d]=\begin{bmatrix}(1-d_f)E_1 & (1-d_f)(1-d_m)\gamma_{21}E_1 & 0\\ (1-d_f)(1-d_m)\gamma_{12}E_2 & (1-d_m)E_2 & 0\\ 0 & 0 & (1-d_s)G_{12}D\end{bmatrix}. \quad (5)$$

Box I

d_f, d_m, and d_s are the current states of fiber damage, matrix damage, and shear damage, respectively. The stacking sequence used for the purpose of analysis is $[0/90]_s$ for GE and JE laminates.

3.3. Details of the FE model

The damage phenomenon that occurs in the present study is highly nonlinear, and ABAQUS/CAE (explicit) is a highly robust software product for such situations. Thus, FE analysis is carried out by ABAQUS/CAE FE software to study the behavior of GE and JE laminates along with JRJ sandwich subjected to the LVI. Eight-node continuum shell elements (SC8R) with Hashin 2D criterion are used to model the laminates. The laminate is modeled as per the ASTM D7136/D7136M standard with a dimension of 0.1 m $\times$ 0.15 m, as shown in Figure 3. In order to reduce the computational time and effort, only quarter plate and impactor are modeled due to their symmetry in nature.

Stiffness hourglass option was used for continuum shell elements. The total thickness of laminate is 0.002 m (2 mm) with each ply measured as 0.0005 m (0.5 mm) for GE and JE laminates and, for JRJ sandwich, the rubber core thickness is maintained as 0.001 m and each facesheet of jute as 0.0005 m. The impact zone was meshed finer (1×1 mm^3) and the remaining regions coarser (1.5×1.5 mm^3) for GE and JE.

The impactor was modeled with rigid shell elements (R3D4) with the reference point at the center of mass where an initial velocity of 2.5 m/s was prescribed. As a part of the interaction property, general contact (explicit) is assigned for the purpose of analysis, where frictionless contact and separation after contact are defined. The boundary conditions of fixed support on four sides of the finer mesh region of the composite plate are considered and, for the two side edges of the laminate, the PINNED boundary condition is considered. For the impactor, the displacement/rotation boundary condition is defined with its movement restricted in U1, U2, UR1, UR2, and UR3 directions and allowing movement only in the U3 direction, which is the Z direction. The assembled view of laminate and impactor along with their meshing is shown in Figure 4 and, for JRJ sandwich, it is shown in Figure 5.

The number of elements used in the analysis is shown in Table 3.

Penalty contact method was used to model the contact between the impactor and the top surface of the laminate, and the general contact method was

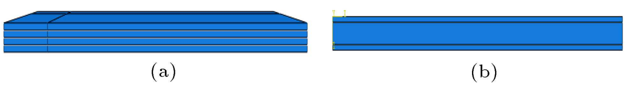

Figure 3. Schematic representation of (a) GE and JE laminates and (b) JRJ sandwich.

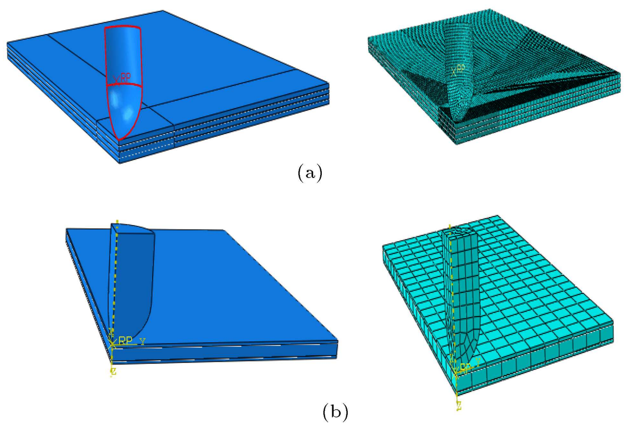

Figure 4. Assembled view of laminate and impactor, meshing for (a) GE and JE laminates and (b) JRJ sandwich.

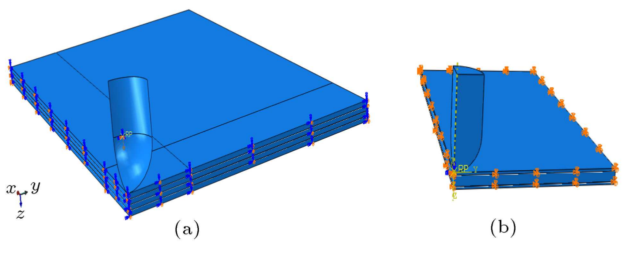

Figure 5. Boundary condition applied to (a) GE and JE laminates and (b) JRJ sandwich.

Table 3. Number of elements used for various parts.

Part	Number of elements
Laminate: Impact zone (finer mesh region)	5,184
Laminate (coarser mesh region)	21,984
Impactor	661
Jute	788
Rubber	1489

used for defining contact between the plies in order to bring them under the general contact domain. A hard contact with pressure over closure and a friction coefficient of 0.3 were used between the impactor and the top laminate, while a friction coefficient of 0.7 was used between different plies based on reported studies [33,34].

4. Results and discussion

4.1. Cohesive surface quadratic stress criterion (CSQUADSCRT) in GE and JE laminates

The cohesive-based surface is used to connect the surfaces of plies in the present work. The cohesive surface quadratic stress criterion (CSQUADSCRT) indicates whether the contact stress damage initiation criterion has been satisfied at the contact point. Whenever CSQUADSCRT = 1, at that point of contact, damage initiation criterion has been satisfied. Figure 6 shows damage initiation for GE and JE, where we can clearly identify the delamination occurring in the case of GE and JE laminates

4.2. Hashin damage parameters for GE and JE laminates

For fiber-reinforced composites, the material damage initiation capability is based on Hashin's theory, and the various Hashin damage initiation criteria used are shown in Figure 7. Based on the fiber compressive initiation criterion (HSNFCCRT) for GE and JE laminates, delamination occurs for GE and JE laminates such that delamination is larger in JE than GE. In addition, fiber failure due to compression is observed in GE more than that in JE laminate. In the case of JE, jute fibers are damaged to a greater extent at the point of the impactor contact, and the damage gradually is reduced towards the tip of laminate, whereas the fiber damage area remains even throughout in the case of GE laminate. According to fiber tensile initiation criterion (HSNFTCRT), it can be observed that the amount of fibers failing in tension is seen at a great degree in GE than JE.

According to the matrix compressive initiation criterion (HSNMCCRT) and matrix tensile initiation criterion (HSNMTCRT), it can be concluded that the failure of matrix by compression and tension is observed more clearly in GE and JE laminates, which can be due to the brittle nature of the laminate, and is more evident at the impact zone than other zones of the laminate. The matrix failure due to tension is almost similar both in GE and JE, except that the matrix failure extends to other regions of JE laminate, but is confined to the impact zone in the case of GE laminate. It can be concluded that the main reason for failure in GE and JE laminates is delamination, as evident in Figure 6.

4.3. Damage behavior of JRJ sandwich

Figure 8 shows the damage behavior of JRJ sandwich. It can be clearly observed that the nature of damage is ductile as opposed to GE and JE laminates, where the nature of damage is brittle. The JRJ sandwich deforms more than GE and JE, thereby absorbing more energy. The reason behind such a behavior of the JRJ sandwich may be the presence of a rubber, which is compliant in nature; thus, the JRJ sandwich is enabled to absorb greater energy. Therefore, flexible composites can absorb more energy than conventional brittle composites.

4.4. Force

Figure 9 shows the comparison of Incipient Point (IP) and Peak Load (PL) for GE, JE, and JRJ laminates. The incipient point for GE, JE, and JRJ is at force rates of 480 N, 310 N, and 0 N, respectively, meaning that the matrix in the case of JRJ, which is the rubber, has not failed as opposed to GE and JE, where the matrix is epoxy. This is due to the ductile and compliant nature of the rubber, and the matrix in JE laminate has failed earlier followed by GE. This statement is supported by the Hashin's failure criterion discussed earlier, where it is evident that matrix cracking has played a vital role in the failure of JE laminate. The peak loads for GE, JE, and JRJ are 580 N, 480 N, and 668 N, respectively.

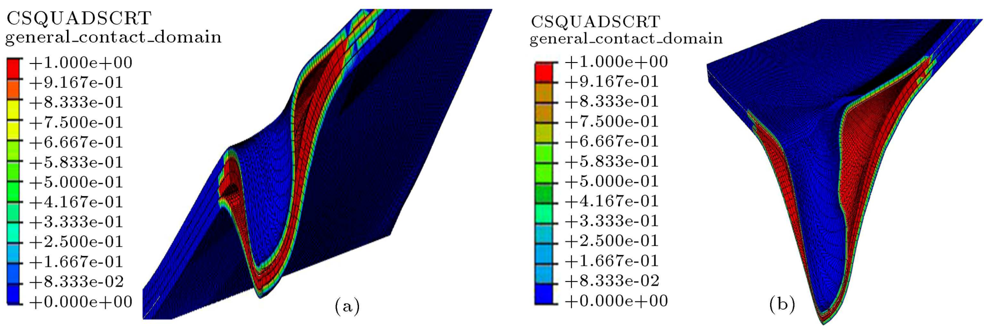

Figure 6. Damage initiation for (a) GE, (b) JE, and (c) JRJ laminate (intended for color reproduction).

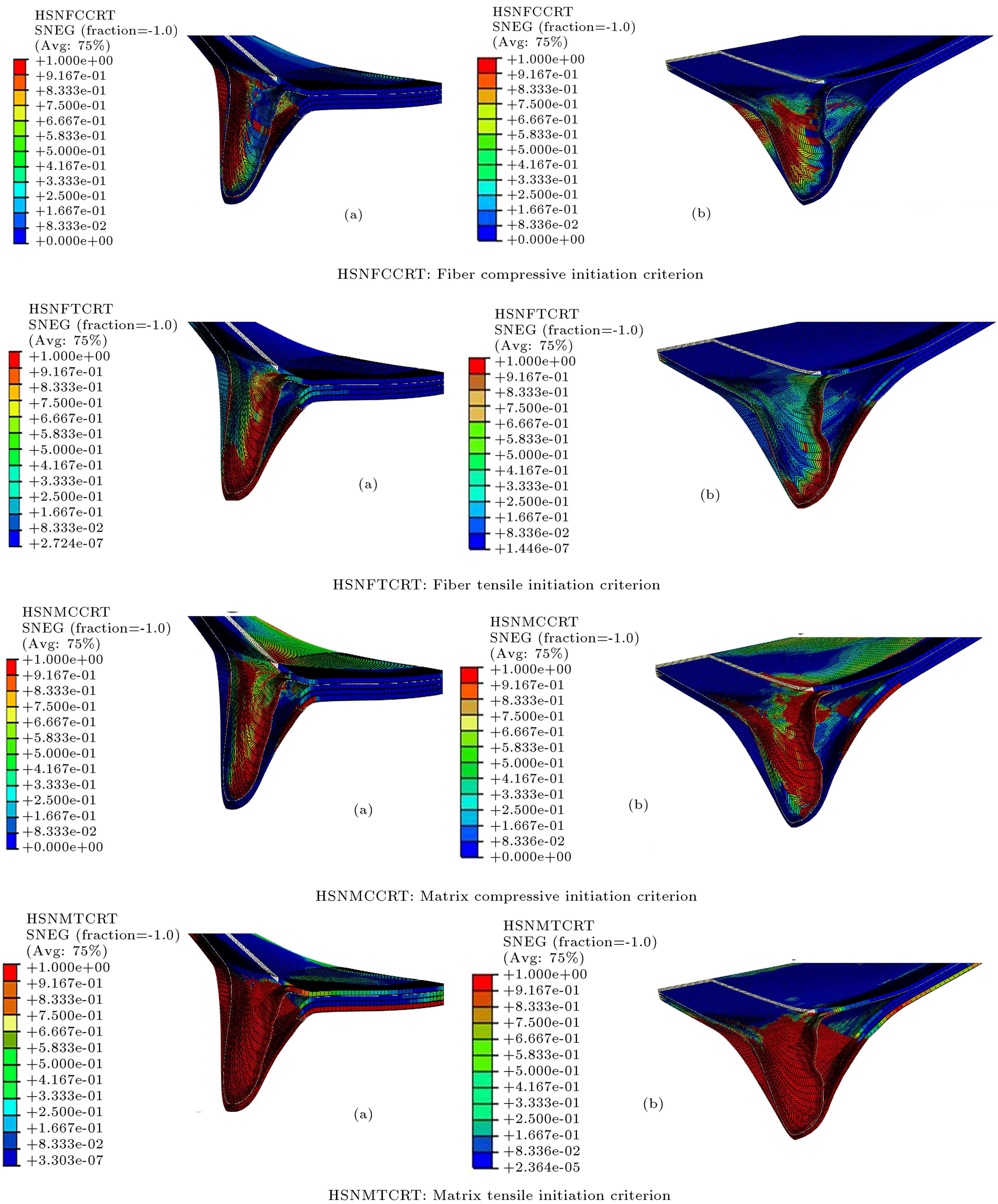

Figure 7. Hashin damage initiation criteria for (a) GE and (b) JE (intended for color reproduction).

4.5. Energy

The energy history for GE, JE, and JRJ laminates is compared, as shown in Figure 10. The impactor transfers all its energy to the laminate and, then, due to the elastic recovery of plate, it rebounds. Because of various damage dissipation phenomena that occur during an impact event, the energy used for recovery has not been seriously compared to impact energy. The energy is dissipated in different failure modes. At the end of the rebound stage, the absorbed energy stabilizes at a particular value. The energies absorbed in the case of GE, JRJ, and JE laminates are 6.3 J,

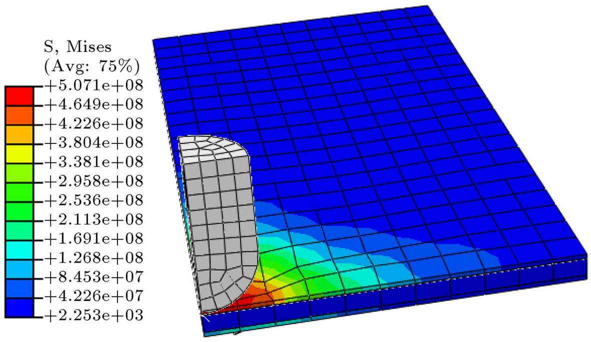

Figure 8. Damage behavior of JRJ sandwich (intended for color reproduction).

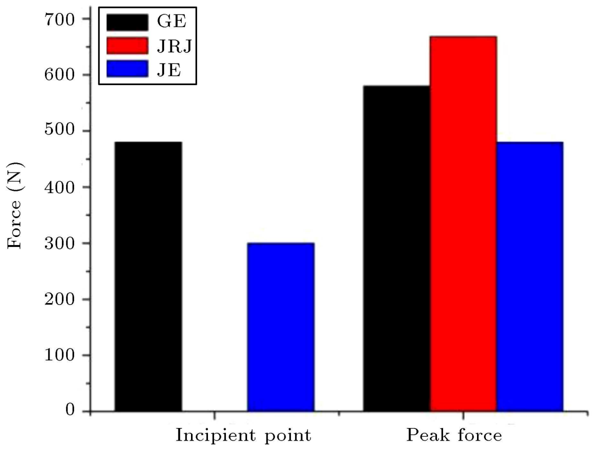

Figure 9. Comparison of incipient point and peak load for GE, JE, and JRJ (intended for color reproduction).

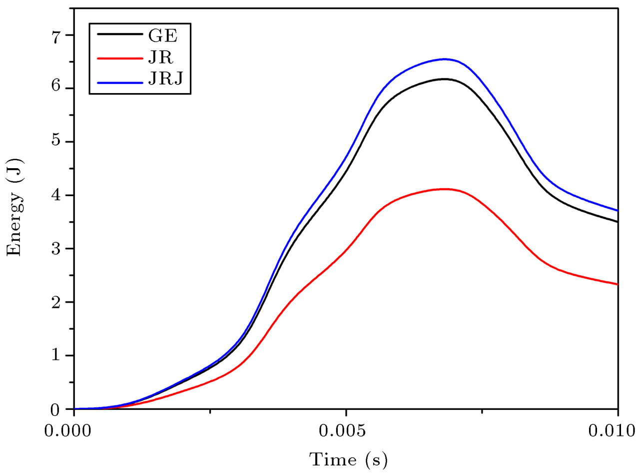

Figure 10. Energy versus time plot for GE, JE, and JRJ (intended for color reproduction).

6.68 J, and 4.2 J, respectively. The energy absorbed by JRJ is superior to that of GE composite.

5. Conclusions

In the present work, the drop-weight impact responses of GE, JE, and JRJ laminate were investigated by FE analysis. Cohesive-based surface was used to connect the surfaces of plies. Hashin's damage criterion (2D) for fiber-reinforced composites readily available in ABAQUS/CAE prompted the current study of the damage behavior of the GE and JE laminates. It was found that delamination occurred in the case of GE and JE laminates with the highest amount of delamination in JE, whereas there was no delamination in the case of JRJ laminate. The failure of matrix by compression and tension was more visible in GE and JE laminates, which can be due to the brittle nature of the laminate, and was more evident at the impact zone than other zones of the laminate, whereas the evidence of matrix failure was found minimal for JRJ laminate. This may be due to the compliant nature of the rubber that can expand, thereby absorbing more energy during Low-Velocity Impact (LVI) loading. The incipient point for JRJ was absent, meaning that the matrix in the case of JRJ, which is the rubber, did not fail as opposed to GE and JE where the matrix was epoxy. This is due to the ductile and compliant nature of the rubber, and the matrix in JE laminate failed earlier, followed by GE. The peak load for JRJ was 1.15 times greater than that for GE and 1.4 times greater than that for JE; the energy absorbed by JRJ was 1.06 times more than that by GE and 1.6 times more than that by JE. JRJ flexible composites were less prone to damage than brittle composites such as JE and GE and, thus, were suitable for LVI applications. The natural fiber in combination with the rubber yields a flexible composite, which is a better energy-absorbing material than brittle composites.

References

1. Friedrich, K. and Almajid, A.A. "Manufacturing aspects of advanced polymer composites for automotive applications", *Applied Composite Materials*, **20**(2), pp. 107-128 (2013).

2. Dogan, A. and Arikan, V. "Low-velocity impact response of E-glass reinforced thermoset and thermoplastic based sandwich composites", *Composites Part B: Engineering*, **127**, pp. 63-69 (2017).

3. Richardson, M.O.W. and Wisheart, M.J. "Review of low-velocity impact properties of composite materials", *Composites Part A: Applied Science and Manufacturing*, **27**(12), pp. 1123-1131 (1996).

4. Jang, B.W. and Kim, C.G. "Real-time detection of low-velocity impact-induced delamination onset in composite laminates for efficient management of structural health", *Composites Part B: Engineering*, **123**, pp. 124-135 (2017).

5. Yang, B., Wang, Z., Zhou, L., Zhang, J., and Liang, W. "Experimental and numerical investigation of interply hybrid composites based on woven fabrics and PCBT resin subjected to low-velocity impact", *Composite Structures*, **132**, pp. 464-476 (2015).

6. Yang, B., Wang, Z., Zhou, L., Zhang, J., Tong, L., and Liang, W. "Study on the low-velocity impact response and CAI behavior of foam-filled sandwich panels with hybrid facesheet", *Composite Structures*, **132**, pp. 1129-1140 (2015).
7. Wu, J., Liu, X., Zhou, H., Li, L., and Liu, Z. "Experimental and numerical study on soft-hard-soft (SHS) cement based composite system under multiple impact loads", *Materials and Design*, **139**, pp. 234-257 (2018).
8. Yang, B., He, L., and Gao, Y. "Simulation on impact response of FMLs: effect of fiber stacking sequence, thickness, and incident angle", *Science and Engineering of Composite Materials*, **25**(3), pp. 621-631 (2017).
9. Zhang, C., Duodu, E.A., and Gu, J. "Finite element modeling of damage development in cross-ply composite laminates subjected to low velocity impact", *Composite Structures*, **173**, pp. 219-227 (2017).
10. Abir, M.R., Tay, T.E., Ridha, M., and Lee, H.P. "On the relationship between failure mechanism and Compression After Impact (CAI) strength in composites", *Composite Structures*, **182**, pp. 242-250 (2017).
11. Kling, S. and Czigany, T. "Damage detection and self-repair in hollow glass fiber fabric reinforced epoxy composites via fiber filling", *Composites Science and Technology*, **99**, pp. 82-88 (2014).
12. Wang, Z., Xu, L., Sun, X., Shi, M., and Liu, J. "Fatigue behavior of glass-fiber-reinforced epoxy composites embedded with shape memory alloy wires", *Composite Structures*, **178**, pp. 311-319 (2017).
13. Almansour, F.A., Dhakal, H.N., and Zhang, Z.Y. "Effect of water absorption on Mode I interlaminar fracture toughness of flax/basalt reinforced vinyl ester hybrid composites", *Composite Structures*, **168**, pp. 813-825 (2017).
14. Wang, S., Huang, L., An, Q., Geng, L., and Liu, B. "Dramatically enhanced impact toughness of two-scale laminate-network structured composites", *Materials and Design*, **140**, pp. 163-171 (2018).
15. Zhandarov, S. and Mader, E. "Determining the interfacial toughness from force-displacement curves in the pull-out and microbond tests using the alternative method", *International Journal of Adhesion and Adhesives*, **65**, pp. 11-18 (2016).
16. Zheng, N., Huang, Y., Liu, H.Y., Gao, J., and Mai, Y.W. "Improvement of interlaminar fracture toughness in carbon fiber/epoxy composites with carbon nanotubes/polysulfone interleaves", *Composites Science and Technology*, **140**, pp. 8-15 (2017).
17. Sonnenfeld, C., Jakani, H.M., Agogue, R., Nunez, P., and Beauchene, P. "Thermoplastic/thermoset multilayer composites: A way to improve the impact damage tolerance of thermosetting resin matrix composites", *Composite Structures*, **171**, pp. 298-305 (2017).
18. Wambua, P., Ivens, I., and Verpoest, I. "Natural fibers: can they replace glass in fibre reinforced plastics?", *Composites Science and Technology*, **63**(9), pp. 1259-1264 (2003).
19. Monteiro, S.N., Lopes, F.P.D., Ferreira, A.S., and Nascimento, D.C.O. "Natural fiber polymer matrix composites: cheaper, tougher and environmentally friendly", *JOM*, **61**(1), pp. 17-22 (2009).
20. Holbery, J. and Houston, D. "Natural-fiber-reinforced polymer composites applications in automotive", *JOM*, **58**(11), pp. 80-86 (2006).
21. Thomas, N., Paul, S.A., Pothan, L.A., and Deepa, B., *Natural Fibers: Structure, Properties and Applications*, Springer-Verlag Publications, Berlin, pp. 3-42 (2011).
22. Satyanarayana, K.G., Guimaraes, J.L., and Wypych, F. "Studies on lingo cellulosic fibers of Brazil. Part I: Source, production, morphology, properties and applications", *Composites Part A Applied Science and Manufacturing*, **38**(7), pp. 1694-1709 (2007).
23. Ariatapeh, M.Y., Mashayekhi, M., and Rad, S.Z. "Prediction of all-steel CNG cylinder fracture under impact using a damage mechanics approach", *Scientia Iranica, Transactions B*, **21**(3), pp. 609-619 (2014).
24. Vishwas, M., Joladarashi, Sh., and Kulkarni, S.M. "Investigation on effect of using rubber as core material in sandwich composite plate subjected to low velocity normal and oblique impact loading", *Scientia Iranica, Transactions B*, **26**(2), pp. 897-907 (2019). DOI: 10.24200/sci.2018.5538.1331
25. Karas, K. "Plates under lateral impact", *Archive of Applied Mechanics*, **10**, pp. 237-250 (1939).
26. Hyunbum, P. "Investigation on low velocity impact behavior between graphite/epoxy composite and steel plate", *Composite Structures*, **171**, pp. 126-130 (2017).
27. Khan, S.H., Sharma, A.P., and Parameswaran, V. "An Impact induced damage in composite laminates with intra-layer and inter-laminate damage", *Procedia Engineering*, **173**, pp. 409-416 (2017).
28. Zhang, C., Duodu, E.A., and Gu, J. "Finite element modeling of damage development in cross-ply composite laminates subjected to low velocity impact", *Composite Structures*, **173**, pp. 219-227 (2017).
29. Rajole, S., Kumar, N., Ravishankar, K.S., and Kulkarni, S.M. "Mechanical characterization and finite element analysis of jute-epoxy composite", *MATEC Web of Conferences*, **144** (2018).
30. Lee, S.M., *Handbook of Composite Reinforcement*, Wiley publications, Palo Alto, California, USA (1992).
31. Mir, A., Aribi, C., and Bezzazi, B. "Study of the green composite jute/epoxy", *International Journal of Chemical, Molecular, Nuclear, Materials and Metallurgical Engineering*, **8**(2), pp. 182-186 (2014).
32. Hossain, M.R., Islam, M.A., Vuurea, A.V., and Verpoest, I. "Effect of fiber orientation on the tensile properties of jute epoxy laminated composite", *Journal of Scientific Research*, **5**(1), pp. 43-54 (2013).

33. Lopes, C.S., Camanho, P.P., Grdal, Z., Maim, P., and Gonzlez, E.V. "Low-velocity impact damage on dispersed stacking sequence laminates. Part II: Numerical simulations", *Composites Science and Technology*, **69**(7-8), pp. 937-947 (2009).

34. Schn, J. "Coefficient of friction of composite delamination surfaces", *Wear*, **237**(1), pp. 77-89 (2000).

Biographies

Vishwas Mahesh received his B.E degree in Mechanical Engineering and M.Tech degree in Product Design and Manufacturing in 2007 and 2011, respectively, from Visvesvaraya Technological University, Belagavi, Karnataka, India. He is currently working as a Research Scholar at the Department of Mechanical Engineering, National Institute of Technology Karnataka, Surathkal, Mangalore, India. His research interests include composite materials and impact dynamics. He has published and presented many papers in international journals and conferences.

Sharnappa Joladarashi received his B.Eng. degree in Mechanical Engineering and M.Eng. degree in Advanced Manufacturing Engineering in 2000 and 2003, respectively, from Gulbarga University, Karnataka, India and National Institute of Technology Karnataka, Surathkal. He has also received his PhD degree from the Indian Institute of Technology Madras (IIT-M) in 2008. He is currently working as an Assistant Professor at the Department of Mechanical Engineering, National Institute of Technology Karnataka, Surathkal, Mangalore, India. His research interests include composite materials. He has published and presented many papers in international journals and conferences.

Satyabodh M Kulkarni received his B.Eng. degree in Mechanical Engineering and M.Eng. degree in Mechanical Engineering in 1985 and 1989, respectively, from Mysore University, Karnataka, India and Bharthiar University, Tamilnadu, India. He has also received his PhD degree from the Indian Institute of Science Bangalore (IISc) in 2002. He is currently working as a Professor at the Department of Mechanical Engineering, National Institute of Technology Karnataka, Surathkal, Mangalore, India. His research interests include composite materials, MEMS. He has published and presented many papers in international journals and conferences and also authored many book chapters.